Shifted shock-fitting: a new paradigm to handle shock waves for Euler equations

Mirco Ciallella, Mario Ricchiuto, Renato Paciorri, Aldo Bonfiglioli

Italian Association of Aeronautics and Astronautics
XXV International Congress
9-12 September 2019| Rome, Italy

SHIFTED SHOCK-FITTING: A NEW PARADIGM TO HANDLE SHOCK WAVES FOR EULER EQUATIONS

M. Ciallella[1*], M. Ricchiuto[2], R. Paciorri[1] , and A. Bonfiglioli[3]

[1]Dipartimento di Ingegneria Meccanica e Aerospaziale, Universitá degli Studi di Roma "La Sapienza", Via Eudossiana 18, 00184 Rome, Italy
*e-mail: mirco.ciallella@gmail.com

[2]Team CARDAMOM, INRIA Bordeaux Sud-Ouest, 33405 Talence, France

[3]Scuola di Ingegneria, Universitá della Basilicata, Via dell'Ateneo Lucano 10, 85100 Potenza, Italy

ABSTRACT

A novel shock-fitting technique, named "shifted shock-fitting", has been implemented on two-dimensional unstructured grids to deal with shocks by treating them as they were immersed boundary. The new algorithm is aimed at coupling a floating shock-fitting technique with the shifted boundary method, so far introduced only to simulate flows with embedded boundaries.

Keywords: Shock-fitting, unstructured mesh, embedded-boundary

1 INTRODUCTION

This paper is concerned with the numerical approximation of solutions of the compressible Euler equations for a perfect gas. In high speed applications the flow develops strong shocks whose numerical approximation is quite challenging, and prone to the introduction of spurious effects related to the structure of the numerical dissipation on a given mesh topology.

To mitigate these effects, we consider a numerical method evolving an explicit discretization of the manifold describing the discontinuity. In particular, given an unstructured discretization of the spatial domain, the CFD mesh, an initial approximation of the flow variables on this mesh, and an initial discretization of the shock surface, we proceed in three steps:

1. Coupling: coupling of shock-CFD mesh, and definition of separate computational domains;

2. CFD iteration: evolving in time the flow variables in each computational domain;

3. Shock update: evolution of position and flow variables of shock-points.

These 3 steps are common to other shock-fitting type approaches, and in particular the unstructured grid shock-fitting method proposed in [12]. The latter has been validated on several complex cases both in two and three space dimensions [3, 11, 13]. The most critical ingredient for this method are steps 1 and 3. In the original method by [12] the approach used is to perform

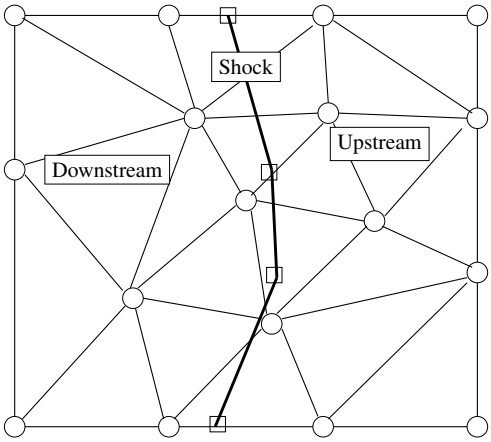

Figure 1: Shock front moving over the CFD mesh

some form of local re-meshing allowing to include all the faces of the shock mesh as faces of the CFD one. This re-meshing phase accomplished, the flow variables need to be appropriately interpolated on the new mesh. Note that, in the context of collocated numerical methods with unknowns on mesh faces, all flow variables are twice stored and solved for in correspondence of the shock. While now quite well validated, this approach has a main drawback in the need of robust and possibly time consuming re-meshing techniques. This may present some issues in terms of constrained re-meshing for a given size of the shock mesh, as well as in terms of efficiency, especially in parallel computations, and especially in three space dimensions.

The main contribution of this work is to propose an approach to alleviate the constraint of having to insert exactly the shock mesh into the CFD one. To this end, we exploit ideas coming from embedded computational methods. We use an extrapolation technique based on the *shifted boundary method* proposed initially in [8, 9] for elliptic problems, and extended to embed boundary conditions in hyperbolic problems in [15]. So the new method proposed consists in defining sufficiently accurate extrapolation functions, to transfer the information to and from the shock mesh. This allows to completely remove the need of re-meshing. In the next sections we present in some detail this new *shifted shock fitting* (SSF) method, and discuss representative flow computations showing its accuracy, and its potential to handle complex shock configurations.

2 Shifted shock-fitting algorithm

To describe the main elements of the SSF method, consider a two-dimensional domain crossed at time t by a shock, as in Fig. 1. The CFD mesh is composed by triangular elements with nodes denoted by circles, while the shock, whose position is completely independent on the CFD mesh, is represented by a polyline. We assume that at time t the solution is known at all grid and shock points. The steps to obtain the solution at $t+\Delta t$ are detailed below. Note that supersonic inflow conditions are assumed.

2.1 Cell removal around the shock front

As in [12], first we flag the grid elements crossed by the shock. This generates a cavity within the CFD mesh that, contrary to [12], is not re-meshed. This cavity separates two computational domains, one upstream of the shock, one downstream. The boundaries of the cavity define *surrogate* shock surfaces, in red in Fig. 2, which are the boundaries of the new computational domains closest to the shock. These are denoted as $\tilde{\Gamma}_U$ and $\tilde{\Gamma}_D$. A second downstream surrogate

boundary, denoted by $\hat{\Gamma}_D$ and in blue in Fig. 2, is created by removing the cells with at least one node on $\tilde{\Gamma}_D$. We also denote by Γ_U and Γ_D the limit of the shock from the right, and from the left respectively. Although geometrically these two coincide, the associated solutions do not.

Along each of these boundaries, we compute tangent and normal unit vectors using the finite difference rules introduced in [12].

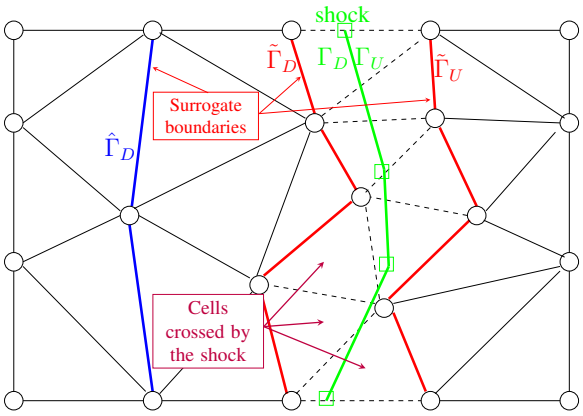

Figure 2: Cell removal across the shock polyline

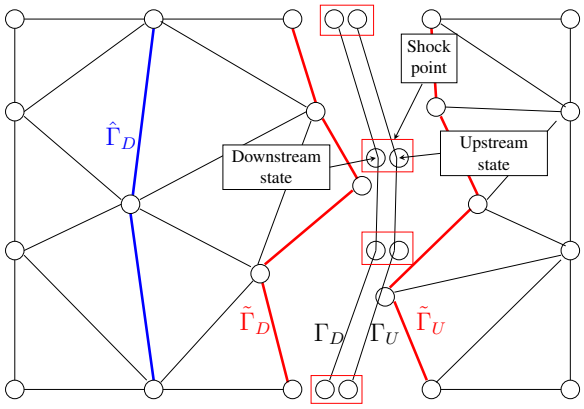

Figure 3: Definition of surrogate and shock boundaries

2.2 Solution update using the CFD solver

To update the solution in the nodes of the CFD mesh, we use an unstructured code based on Residual Distribution [1,7], and in particular using a multidimensional upwind shock-capturing variant of the method [2,4]. Two independent runs of the CFD solver are used to evolve to $t+\Delta t$ the solution values in the domains separated by the cavity, the upstream one, with $\tilde{\Gamma}_U$ as one of the boundaries, and the downstream one, whose boundary contains $\tilde{\Gamma}_D$. For supersonic inflow conditions, the nodes on $\tilde{\Gamma}_U$ are correctly updated, whereas the nodes on $\tilde{\Gamma}_D$ are not correct, since they do not account for the waves coming from the shock (right-running acoustic wave, entropy wave and vorticity wave). The shock points on Γ_U and Γ_D also need to be updated.

To correct the points on $\tilde{\Gamma}_D$, and to update the solution values on the shock we need to define appropriate functions to transfer solution values to/from different boundaries. In particular, we will transfer values of the computed Roe's parameter vector, and we will re-use the downstream Riemann variable, associated to the left-running acoustic wave:

$$R_D^{t+\Delta t} = \tilde{a}^{t+\Delta t} + \frac{\gamma-1}{2}\,\tilde{\vec{u}}_d^{t+\Delta t}\cdot\vec{n} \tag{1}$$

where $\vec{n}$ is the shock normal, $\tilde{a}^{t+\Delta t}$ is the speed of sound and $\tilde{\vec{u}}_d^{t+\Delta t}$ is the flow velocity. Note that, $R_d^{t+\Delta t}$ can be assumed to be correct, even though individually $\tilde{a}^{t+\Delta t}$ and $\tilde{\vec{u}}_d^{t+\Delta t}$ may not be.

2.3 First transfer of the Roe's parameter vector

The solution transfer is used to update values on the upstream side of the shock Γ_U, and to transport $R_D^{t+\Delta t}$ from $\tilde{\Gamma}_D$ to Γ_D. Following [15], we use a Taylor expansion truncated to the second order

$$\phi(\boldsymbol{x}) = \phi(\tilde{\boldsymbol{x}}) + \nabla\phi(\tilde{\boldsymbol{x}})\cdot(\boldsymbol{x}-\tilde{\boldsymbol{x}}) + o(\|\boldsymbol{x}-\tilde{\boldsymbol{x}}\|^2) \tag{2}$$

where ϕ is a generic variable, $\boldsymbol{x}$ and $\tilde{\boldsymbol{x}}$ are the node coordinates that respectively belong to Γ and $\tilde{\Gamma}$ and, $\nabla\phi(\tilde{\boldsymbol{x}})$ is the gradient computed on the surrogate boundary, obtained by means of a one sided Green-Gauss formula. In practice, the transfer is performed as follows.

Upstream: from the surrogate boundary $\tilde{\Gamma}_U$ to the shock boundary Γ_U
To be consistent with the physics of the problem, the map $\tilde{\mathbf{x}} \rightarrow \mathbf{x}$ is parallel to the shock normal in the point that has to be updated. As shown on Fig. 4, the position of the intersection point A^i allows to define the interpolated state using the solution in the two neighbouring nodes as :

$$\phi(A^i) \;=\; \phi(A_1^i) \cdot w_2 \;+\; \phi(A_2^i) \cdot w_1 \tag{3}$$

This interpolated value is transferred using (2), with $\boldsymbol{x}$ the position of shock point, and $\tilde{\boldsymbol{x}} = A^i$.

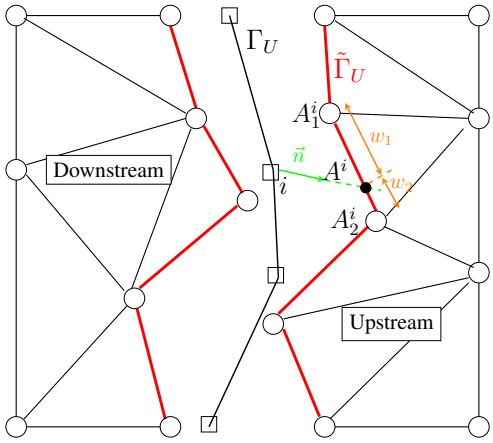

Figure 4: Transport of variables from $\tilde{\Gamma}_U$ to Γ_U

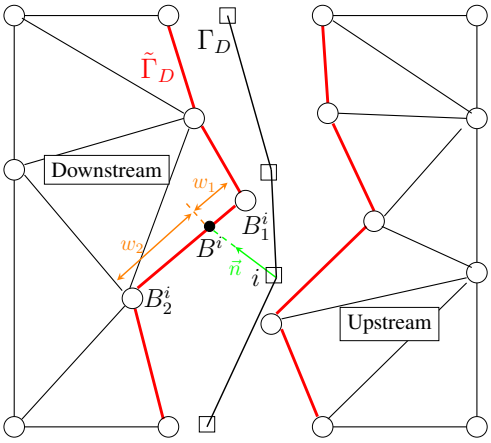

Figure 5: Transport of variables from $\tilde{\Gamma}_D$ to Γ_D

Downstream: from the surrogate boundary $\tilde{\Gamma}_D$ to the shock boundary Γ_D
The Riemann variable (1) is transferred from $\tilde{\Gamma}_D$ to Γ_D using (2). As for the upstream boundaries, the transfer is performed between the shock point and a point B^i on the surrogate, mapped in the direction of the shock normal.

2.4 Shock calculation

The correct downstream state, along with the shock speed in each shock point, is computed by using the Rankine-Hugoniot jump relations. Details about this step can be found in Ref. [12]

2.5 Second transfer of the Roe's parameter vector

The second transfer allows to correct the solution values in the nodes on $\tilde{\Gamma}_D$. To do this, we map the surrogate boundary nodes onto the shock, as shown on Fig. 6. The variables in the mapped point S^i are interpolated using the neighbouring nodes S_1^i and S_2^i. To avoid using the incorrect nodal values in the gradient evaluation, we use the second surrogate $\hat{\Gamma}_D$ (see Fig. 2) to interpolate the mapped shock value in the surrogate point. In particular, to compute the solution in i, we perform a linear interpolation in the triangle, where i falls, defined by the shock point S^i and two points on $\hat{\Gamma}_D$.

2.6 Shock displacement

The new position of the shock front at time level $t+\Delta t$ is computed by displacing all discontinuity points employing the following first-order formula:

$$P^{t+\Delta t} \;=\; P^t \;+\; \vec{w}^{\,t+\Delta t}\, \vec{n}\, \Delta t \tag{4}$$

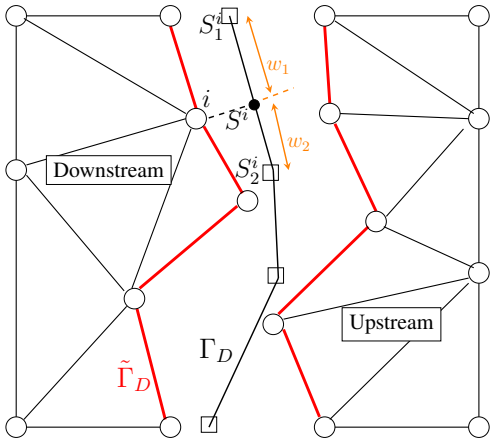

Figure 6: Map from surrogate to shock boundaries

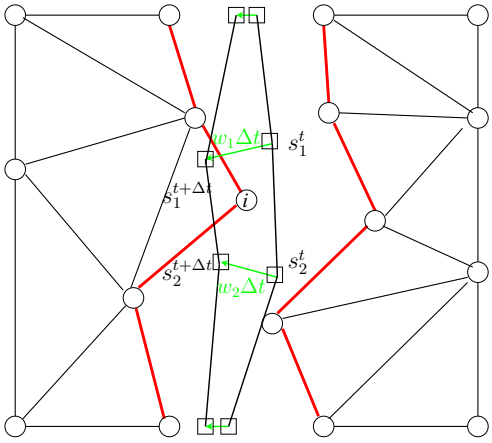

Figure 7: CFD mesh point swept by the shock

where P denotes the shock point position, and the speed w is obtained form the Rankine-Hugoniot relations as discussed in [12]. The above formula is only first order in time, which is enough if only steady flows are considered as in this paper.

2.7 Interpolation of the jumped nodes

Finally, the last step of the algorithm concerns the interpolation of those grid-points that have been swept by the shock front and have passed from one domain to the other. To detect these points, the position of the closest shock edge before and after the displacement, is used to build a quadrilateral, as shown in Fig. 7. If the grid-point i falls inside the quadrilateral composed of points s_1^t, s_2^t, $s_1^{t+\Delta t}$ and $s_2^{t+\Delta t}$, the point state has to be updated.

3 Applications

3.1 Planar source flow

This test-case consists in a compressible, planar source flow that has already been addressed elsewhere [5,6] as a validation case, due to the availability of an analytical solution. Indeed, the radial distribution of the flow variables is identical to that of a Q1D variable-area nozzle flow whereby the area ratio is replaced by the ratio between the radial distance from the source and that of the critical section.

The computational domain consists in the annulus sketched in Fig. 8(a): the ratio between the radii of the outer and inner circles has been set equal to $r_{out}/r_{in} = 2$. A transonic (shocked) flow has been studied by imposing a supersonic inlet flow at $M = 2$ on the inner circle and a ratio between the outlet static and inlet total pressures such that a shock forms at $r_{sh}/r_{in} = 1.5$. The Delaunay mesh used for the simulation has been generated using TRIANGLE [14]; it is made of 27288 grid-points and 53824 triangles.

Figure 8(b) shows a comparison between the SC and SSF solutions, both in terms of entropy, $S = p\rho^{-\gamma}$ and $\sqrt{\rho}u$ isolines. Both flow variables clearly reveal that the SC solution is plagued by severe spurious errors due to the misalignment between the mesh and the "captured" shock.

Moreover, although not reported here, a grid-convergence analysis shows that the discretization error of the SSF solution decreases quadratically also downstream of the shock, whereas the SC solution only exhibits first-order convergence.

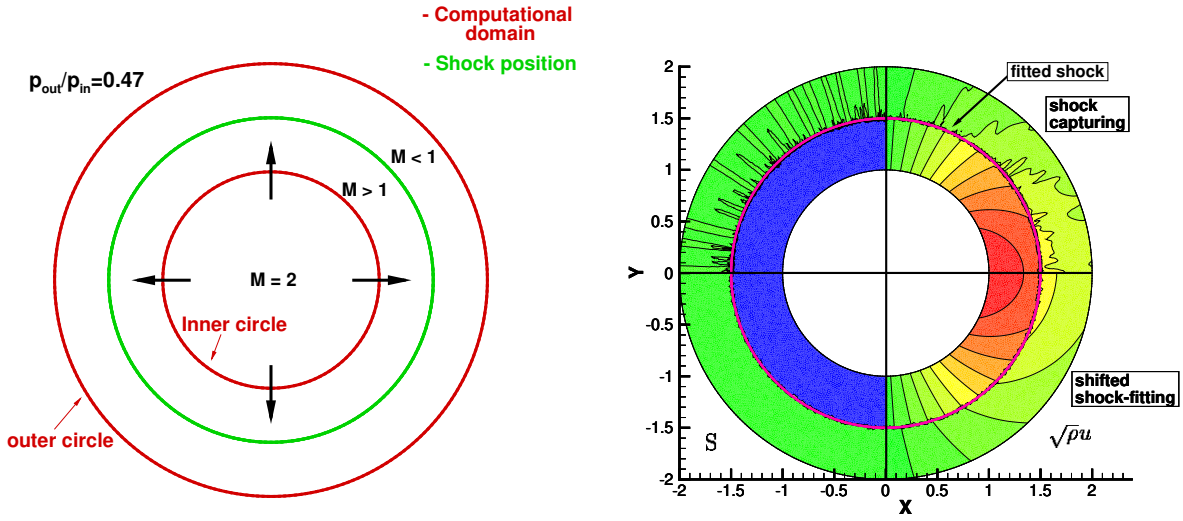

(a) Computational domain and boundary conditions.

(b) Entropy, S, in the 2^{nd} and 3^{rd} quadrant and $\sqrt{\rho}u$ isolines in the 1^{st} and 4^{th} quadrant.

Figure 8: Planar source flow: sketch of the computational domain; comparison between SC (1^{st} and 2^{nd} quadrant) and SSF (3^{rd} and 4^{th} quadrant).

3.2 Steady Mach reflection

One of the key advantages of unstructured shock-fitting over its structured-grid ancestors is its capability [13] to apply the jump relations not only along the various discontinuities, but also within those (intersection) points where different discontinuities eventually meet. This capability is not yet available in the SSF algorithm, which is however capable of operating in a hybrid mode, whereby some of the discontinuities are fitted while others are captured. The present test-case, which consists in a steady Mach reflection, allows to highlight the fact that a remarkable improvement in solution quality over a fully captured simulation is possible even if only some of the discontinuities are fitted. As shown in Fig. 9(a), a uniform, supersonic ($M_\infty = 2$) stream of air undergoes a of $\Theta = 14°$ deflection through an oblique shock (hereafter referred to as the incident shock). For the given free-stream Mach number and flow deflection through the incident shock, a regular shock-reflection is impossible, but a Mach reflection takes place. A Mach reflection consists in a triple point that connects four different discontinuities: the incident and the reflected shocks, the Mach stem and a contact discontinuity.

The computational mesh employed to carry out the SC simulation and also as background triangulation in the SSF simulation was generated with DELAUNDO, a frontal-Delaunay mesh generator [10]; it is characterized by 14833 grid-points and 29214 triangles.

In the hybrid SSF simulation the Mach stem and the reflected shock have been fitted, whereas the incident shock and the contact discontinuity have been captured. An overall view of the Mach isocontours lines and a detail of the triple-point region are shown in Fig. 9. Even though not all the discontinuities that meet at the triple-point have been fitted, the hybrid SSF simulation reveals a much smoother Mach-number distribution, when compared to SC, downstream of both the Mach stem and the reflected shock.

4 CONCLUSIONS

A novel shock-fitting, based on the shifted boundary method, was proposed and applied to several cases. This new technique seems to lead to further simplifications in the development

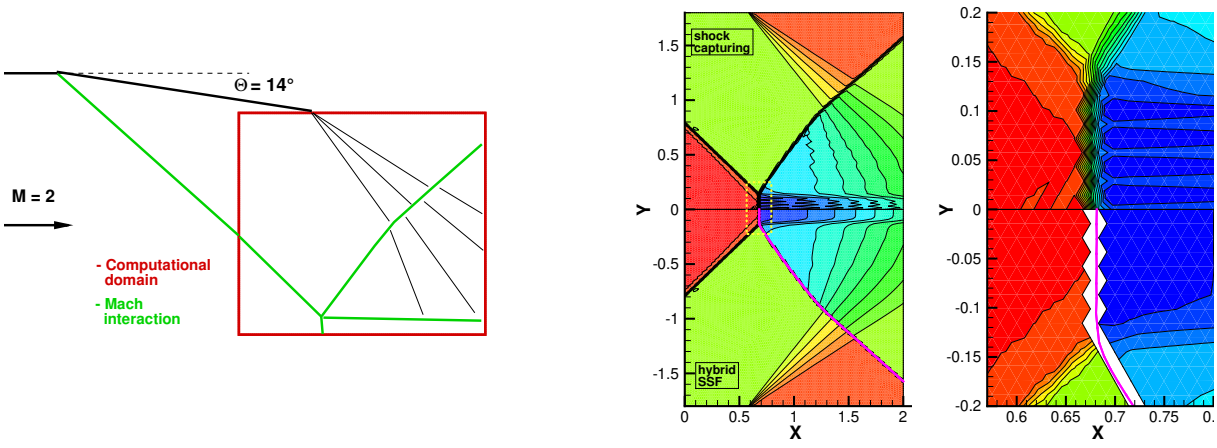

(a) Sketch of the flow topology.

(b) Overall view.

(c) Detail of the triple-point region.

Figure 9: Steady Mach reflection: comparison between the Mach number isocontours computed by means of SC (upper frames) and SSF (lower frames); the fitted shock is shown using a bold solid line.

of shock-fitting techniques because it removes the need of re-generating locally the grid in the proximity of the fitted shock.

REFERENCES

[1] R. Abgrall and M. Ricchiuto. *High-Order Methods for CFD*, pages 1–54. John Wiley & Sons, Ltd., 2017.

[2] Aldo Bonfiglioli. Fluctuation splitting schemes for the compressible and incompressible Euler and Navier-Stokes equations. *International Journal of Computational Fluid Dynamics*, 14(1):21–39, 2000.

[3] Aldo Bonfiglioli, Marco Grottadaurea, Renato Paciorri, and Filippo Sabetta. An unstructured, three-dimensional, shock-fitting solver for hypersonic flows. *Computers & Fluids*, 73:162–174, 2013.

[4] Aldo Bonfiglioli and Renato Paciorri. A mass-matrix formulation of unsteady fluctuation splitting schemes consistent with Roe's parameter vector. *International Journal of Computational Fluid Dynamics*, 27(4-5):210–227, 2013.

[5] Aldo Bonfiglioli and Renato Paciorri. Convergence analysis of shock-capturing and shock-fitting solutions on unstructured grids. *AIAA journal*, 52(7):1404–1416, 2014.

[6] M. Sergio Campobasso and Mohammad H. Baba-Ahmadi. Ad-Hoc Boundary Conditions for CFD Analyses of Turbomachinery Problems With Strong Flow Gradients at Farfield Boundaries. *Journal of Turbomachinery*, 133(4):041010–041010–9, April 2011.

[7] H. Deconinck and M. Ricchiuto. *Residual Distribution Schemes: Foundations and Analysis*, pages 1–53. John Wiley & Sons, Ltd., 2017.

[8] A Main and G Scovazzi. The shifted boundary method for embedded domain computations. Part I: Poisson and Stokes problem. *Journal of Computational Physics*, 372:972–995, 2018.

[9] Alex Main and Guglielmo Scovazzi. The shifted boundary method for embedded domain computations. Part II: Linear advection–diffusion and incompressible Navier–Stokes equations. *Journal of Computational Physics*, 372:996–1026, 2018.

[10] J-D Müller, Philip L Roe, and H Deconinck. A frontal approach for internal node generation in Delaunay triangulations. *International Journal for Numerical Methods in Fluids*, 17(3):241–255, 1993.

[11] Marcello Onofri and Renato Paciorri. *Shock Fitting: Classical Techniques, Recent Developments, and Memoirs of Gino Moretti*. Springer, 2017.

[12] Renato Paciorri and Aldo Bonfiglioli. A shock-fitting technique for 2D unstructured grids. *Computers & Fluids*, 38(3):715–726, 2009.

[13] Renato Paciorri and Aldo Bonfiglioli. Shock interaction computations on unstructured, two-dimensional grids using a shock-fitting technique. *Journal of Computational Physics*, 230(8):3155–3177, 2011.

[14] Jonathan Richard Shewchuk. Triangle: Engineering a 2D quality mesh generator and Delaunay triangulator. In *Workshop on Applied Computational Geometry*, pages 203–222. 1996.

[15] Ting Song, Alex Main, Guglielmo Scovazzi, and Mario Ricchiuto. The shifted boundary method for hyperbolic systems: Embedded domain computations of linear waves and shallow water flows. *Journal of Computational Physics*, 369:45–79, 2018.